



Article

Structural and Electronic Properties of Cu₃InSe₄

Oluwagbemiga P. Ojo ¹D, Winnie Wong-Ng ²D, Tieyan Chang ³D, Yu-Sheng Chen ³ and George S. Nolas ^{1,*}

- Department of Physics, University of South Florida, Tampa, FL 33620, USA
- Materials Measurement Science Division, National Institute of Standards and Technology, Gaithersburg, MD 20899, USA
- ChemMatCARS, University of Chicago, Argonne, IL 60439, USA
- * Correspondence: gnolas@usf.edu

Abstract: Single crystals of a new ternary chalcogenide Cu_3InSe_4 were obtained by induction melting, allowing for a complete investigation of the crystal structure by employing high-resolution single-crystal synchrotron X-ray diffraction. Cu_3InSe_4 crystallizes in a cubic structure, space group $P\bar{4}3m$, with lattice constant 5.7504(2) Å and a density of 5.426 g/cm³. There are three unique crystallographic sites in the unit cell, with each cation bonded to four Se atoms in a tetrahedral geometry. Electron localization function calculations were employed in investigating the chemical bonding nature and first-principle electronic structure calculations are also presented. The results are discussed in light of the ongoing interest in exploring the structural and electronic properties of new chalcogenide materials.

Keywords: ternary chalcogenide; crystal structure; electronic structure



Citation: Ojo, O.P.; Wong-Ng, W.; Chang, T.; Chen, Y.-S.; Nolas, G.S. Structural and Electronic Properties of Cu₃InSe₄. *Crystals* **2022**, *12*, 1310. https://doi.org/10.3390/ cryst12091310

Academic Editor: Sławomir Grabowski

Received: 12 August 2022 Accepted: 11 September 2022 Published: 17 September 2022

Publisher's Note: MDPI stays neutral with regard to jurisdictional claims in published maps and institutional affiliations.



Copyright: © 2022 by the authors. Licensee MDPI, Basel, Switzerland. This article is an open access article distributed under the terms and conditions of the Creative Commons Attribution (CC BY) license (https://creativecommons.org/licenses/by/4.0/).

1. Introduction

Multinary metal chalcogenides consisting of primarily earth-abundant, low-cost, and non-toxic constituents exhibit physical properties that can be tuned via composition, specific bonding scheme, lattice defects or disorder, and have been investigated for a variety of different applications of interest including thermoelectrics [1–6], photovoltaics [7–10], superconductivity [11–13], and as potential topological insulators [14,15]. The interest in ternary Cu-based compositions has recently intensified in pursuit of commercially viable solar cells [16–18] and thermoelectrics [19–22]. The ternary Cu-In-Se system is of particular interest [23], with a number of compounds possible along the Cu₂Se-InSe₃ tie-line [24,25] such as CuInSe₂ [26,27], Cu₃In₅Se₉ [28], Cu₇In₁₉Se₃₂ [23], CuIn₅Se₈ [25], Cu₂In₄Se₇ [29] and CuIn₃Se₅ [30]. The crystal structure of CuInSe₂ was reported to be either tetragonal with space group $I\overline{4}2m$ [31,32] or cubic, $F\overline{4}3m$ [23,33], where the latter structure can be considered as two interpenetrating face-centered cubic sub-lattices. In the case of Cu₃MSe₄, where M is V, Ta, Nb or Sb, both cubic [34,35] and tetragonal [36,37] structure types were reported.

To the best of our knowledge, the synthesis and crystal structure of Cu_3InSe_4 has not been previously reported. Wei et al. [38] predicted Cu_3InSe_4 to be metallic, with "holes in the valence band", however structural information and details of the electronic structure were not reported. Therefore, we have undertaken to synthesize and investigate the crystal structure and electronic properties of Cu_3InSe_4 . We employed high-resolution single crystal synchrotron measurements to determine the structure of this previously unascertained ternary compound. The structural features and bonding were investigated in detail, including analyses of calculated electron localization, and the electronic properties were obtained using density functional theory. Our results are compared to that of other ternary chalcogenides.

2. Materials and Methods

Single crystals of Cu₃InSe₄ were initially obtained in an attempt to prepare CuFe₂InSe₄, resulting in FeSe as well as the shiny metallic ternary chalcogenide crystals identified as

Crystals **2022**, 12, 1310 2 of 7

Cu₃InSe₄. This procedure was repeated with a stoichiometric ratio of the starting highpurity elements, Cu powder (99.9 % purity, Alfa Aesar, Thermo Fisher Scientific, Ward Hill, MA, USA), In shot (99.99 % purity, Alfa Aesar, Thermo Fisher Scientific, Ward Hill, MA, USA) and Se ingot (99.999 % purity, Alfa Aesar, Thermo Fisher Scientific, Ward Hill, MA, USA) [39]. The elements were placed in a silica ampoule and vacuum-sealed inside a quartz tube, then melted via a water-cooled 3-coil induction (Superior Induction, SI-7KWHF) furnace resulting in an agglomeration of gray Cu₃InSe₄ crystals.

Single-crystal synchrotron measurements were carried out at NSF's ChemMatCARS, Sector 15 of the Advanced Photon Source, Argonne National Laboratory. Data were collected using a Huber 3-circle diffractometer (Huber diffraction, Lancaster, CA, USA) equipped with a Pilatus3X 2M detector (Dectris USA Inc., Philadelphia, PA, USA) using an Oxford Cryojet (American Laboratory Trading, East Lyme, CT, USA). The ω -angle was set at -180° , κ -angle was set at 0° and 30° , with ϕ -angle scanned over the range of 360° using the shutterless mode of the detector. Data integration was performed with the Bruker APEX 3 suite software. The reduction of the data was obtained with the SAINT v.8.38A and SADABS v.2016 programs (Bruker AXS Inc., Madison, WI, USA) that are included in the APEX suite. The structure was solved directly and refined by the full-matrix least-squares method.

Ab initio calculations based on density functional theory, plane-waves basis set, and pseudopotentials were carried out using the Quantum Espresso software package [40]. Projector-augmented waves (PAW) pseudopotentials [41], the generalized gradient approximation of Perdew-Burke-Ernzehof [42,43] plus Hubbard correction [44] (GGA-PBE + U) exchange-correlation functional were applied. A U parameter of 4 eV for the cations was used based on previous studies on Cu-based chalcogenide materials [45,46] that provide for good agreement between calculated and experimental structure values. For the pseudopotentials, Cu $3d^{10}4s^{1}$, In $4d^{10}5s^{2}5p^{1}$ and Se $4s^{2}4p^{4}$ valence configurations were considered. For self-consistent field (SCF) calculations, a k-point mesh of $6 \times 6 \times 6$ was applied to sample the Brillouin zone. The kinetic energy cutoff for wavefunctions and charge density was set to 70 Ry and 300 Ry, respectively, and an energy convergence threshold of 10^{-7} eV was utilized. The electron localization function (ELF) distribution was analyzed and visualized using VESTA v.3.5.8 software [47].

CCDC 2172956 contains the supplementary crystallographic data. These data can be obtained free of charge via https://www.ccdc.cam.ac.uk/structures/search?access=referee&pid=ccdc:2172956&author=ng, accessed on 10 September 2022, (or from the CCDC, 12 Union Road, Cambridge CB2 1EZ, UK; Fax: +44 1223 336033; E-mail: deposit@ccdc.cam.ac.uk).

3. Results

The crystallographic data and structural refinement results are shown in Table 1. Cu_3InSe_4 crystallizes in the cubic space group $P\overline{4}3m$ (No. 215) with cell parameter a = 5.7504(2) Å, Z = 1 and density = 5.426 g/cm³. The atomic coordinates and equivalent isotropic displacement parameters, $U_{\rm eq}$, are shown in Table 2. The anisotropic displacement parameters are presented in Table 3. As shown in Figure 1, the structure consists of CuSe₄ (Cu-Se distance of 2.4622(4) Å) and InSe₄ (In-Se distance of 2.5775(13) Å) tetrahedra connected by corner-sharing Se atoms. Selenium is surrounded by three Cu atoms and by an In atom, as shown in Figure 1a. The CuSe₄ and InSe₄ tetrahedra are illustrated in Figure 1b. The tetrahedron about the In site is a regular tetrahedron with Se-In-Se angles of 109.471(11)°, while that of Cu is somewhat distorted with Se-Cu-Se angles ranging from $105.63(6)^{\circ}$ to $111.42(3)^{\circ}$. The Cu-Se distance (2.4622(4) A) is similar to that reported for sulvanite and adamantine compounds [36,48,49], while the In-Se distance (2.5775(13) Å) is similar to that for CuInSe₂ (2.591 Å) [49] and LiInSe₂ (2.57 Å) [50]. It is important to note that the structure of Cu_3InSe_4 is related to that of sulvanites Cu_3XQ_4 (X = V, Nb, Ta; Q = S, Se, Te) [19,51,52]; however, the Cu atoms occupy different Wyckoff sites in these two different ternary chalcogenides thus resulting in corner sharing and edge sharing tetrahedra for Cu₃InSe₄ and Cu₃XQ₄, respectively.

Crystals **2022**, 12, 1310 3 of 7

Table 1.	Crystal	data a	and s	structure	refinement	results.
----------	---------	--------	-------	-----------	------------	----------

Empirical formula	Cu_3InSe_4
Formula weight	621.32
Temperature	100(2) K
Wavelength	0.49594 Å
Crystal system	Cubic
Space group	$P\overline{4}3m$ (No. 215)
Unit cell dimension	a = 5.7504(2)
Volume	190.15(2) \mathring{A}^3
Z	1
Density (calculated)	$5.426 \mathrm{mg/m^3}$
Absorption coefficient	11.36mm^{-1}
Crystal size	$30 \times 20 \times 10 \ \mu\text{m}^3$
Theta range for data collection	2.283 to 26.223°
Reflections collected	2237
Independent reflections	251 [R(int) = 0.0945]
Goodness-of-fit on F^2	1.190
Final R indices $[I > 2\sigma(I)]$	R1 = 0.0375, $wR2 = 0.0886$
R indices (all data)	R1 = 0.0403, $wR2 = 0.0908$

Table 2. Atomic coordinates and equivalent isotropic displacement parameters (Å²). U_{eq} is defined as one third of the trace of the orthogonalized U_{ij} tensor.

Atom	Site	\boldsymbol{x}	\boldsymbol{y}	z	$U_{ m eq}$
In	1b	1/2	1/2	1/2	0.009(1)
Se	4e	0.2412(1)	0.2412(1)	0.2412(1)	0.011(1)
Cu	3 <i>d</i>	0	0	1/2	0.007(1)

Table 3. Anisotropic displacement parameters (Å²). The anisotropic displacement factor exponent takes the form: $-2\pi^2[h^2a^{*2}U_{11} + \ldots + 2hka^*b^*U_{12}]$.

	<i>U</i> ₁₁	U ₂₂	U ₃₃	U_{23}	<i>U</i> ₁₃	U ₁₂
In	0.010(1)	0.010(1)	0.010(1)	0	0	0
Se	0.011(1)	0.011(1)	0.011(1)	-0.002(1)	-0.002(1)	-0.002(1)
Cu	0.007(1)	0.007(1)	0.006(1)	0	0	0

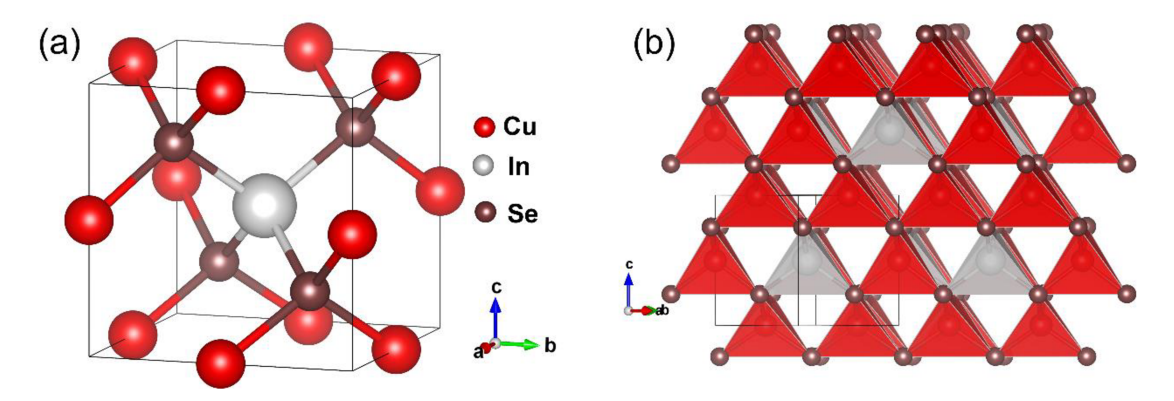


Figure 1. Schematic illustrating the crystal structure of Cu_3InSe_4 showing the (a) unit cell and (b) stacking of the $CuSe_4$ (red) and $InSe_4$ (gray) tetrahedra.

The electron density distribution was investigated by calculating the ELF, revealing the ionic nature of the bonding in Cu_3InSe_4 , as shown in Figure 2. Figure 2 shows the calculated ELF along the (110) plane. ELF values of 0.0, 0.5 and 1.0 represent fully delocalized, electrongas-like pair probability and perfect localization, respectively [53]. The atomic core regions

Crystals **2022**, 12, 1310 4 of 7

of the cations have localization domains with ELF values close to unity and low ELF values away from these regions. This suggests electrons transfer from both Cu and In atoms to adjacent Se atoms, indicating ionic bonding. In comparing the Cu_3XSe_4 compounds [54] with Cu_3InSe_4 , the X-Se bonds in the former show a higher degree of covalency as compared with the primarily ionic character for In-Se in Cu_3InSe_4 .

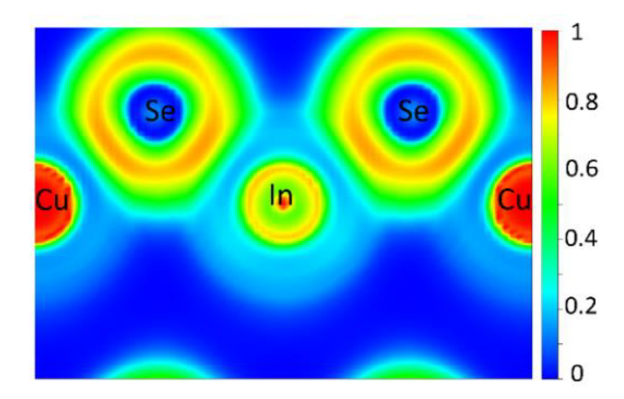


Figure 2. ELF calculated along the (110) plane.

The oxidation states of Cu, In and Se are 1+, 3+ and 2-, respectively, resulting in 30 electrons per formula unit, or two fewer than required for the tetrahedral bonds in Cu₃InSe₄ thus resulting in p-type metallic behavior. Our detailed structural analyses allow for an investigation of the electronic structure of Cu₃InSe₄ by calculating the energy band structure and density of states (DOS). As shown in Figure 3, the Fermi level, E_f , crosses the valence band in multiple regions, thus, Cu_3InSe_4 is a p-type metal [46,55], confirming the simple charge imbalance argument. This is also in agreement with the early conjecture [38], and corroborated by our room temperature conductivity measurements indicating metallic conduction [56]. The orbital-projected DOS indicates that the valence band maximum has contributions mainly from the Cu 3d and Se 4p orbitals, while the conduction band maximum is mainly composed of In 5s and Se 4p and minor contributions from Cu 3d4s4p, In 5p and Se 4s orbitals. The orbital interactions between the CuSe₄ tetrahedra therefore play a dominant role in the metallic conductivity of Cu₃InSe₄. It is instructive to compare the electronic structure of Cu₃InSe₄ to that of Cu₃XSe₄ in light of the fact that the crystal structure of Cu₃InSe₄ is not isostructural to that of the later compositions. Specifically, for the case of the Cu_3XSe_4 compositions [19,57,58], an energy gap opens between the valence and conduction bands in these materials. These compositions are therefore semiconductors and are being investigated for thermoelectric [19,20] and photovoltaic [59,60] applications, whereas in the case of Cu_3InSe_4 E_f falls relatively deep in the valence band and will therefore not be of interest for such applications.

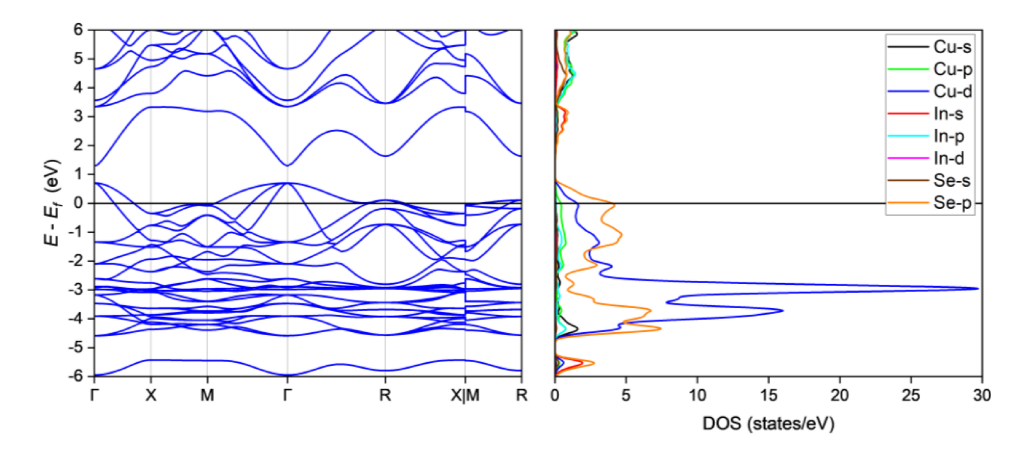


Figure 3. Calculated energy band structure and orbital-projected DOS.

Crystals 2022, 12, 1310 5 of 7

4. Conclusions

Single crystals of a new ternary chalcogenide Cu₃InSe₄ were obtained by induction melting, and the structural and electronic properties are reported for the first time. Cu₃InSe₄ forms in a cubic crystal structure that consists of CuSe₄ and InSe₄ tetrahedra connected by corner sharing Se atoms. Electron localization function analyses indicated partially ionic bonding between the cations and Se atoms, with highly delocalized electrons in the regions between cation and selenium. Electronic structure calculations reveal this ternary chalcogenide to be metallic. Given that ternary chalcogenide compounds are of interest for potential thermoelectric and optoelectronic applications, our findings will be useful for investigations on new materials for applications of interest. The results and analyses in this work add to our understanding of the structural and electronic properties of ternary chalcogenides.

Author Contributions: Conceptualization, G.S.N.; methodology, O.P.O.; data curation, O.P.O., W.W.-N., T.C. and Y.-S.C.; formal analysis, O.P.O., W.W.-N., T.C. and Y.-S.C.; writing—original draft preparation, O.P.O.; writing—review and editing, G.S.N.; visualization, O.P.O.; supervision, G.S.N. All authors have read and agreed to the published version of the manuscript.

Funding: This work was supported, in part, by the National Science Foundation, Grant No. DMR-1748188. W.W.-N., T.C. and Y.-S.C. gratefully acknowledge NSF's ChemMatCARS Sector 15 which is supported by the Divisions of Chemistry (CHE) and Materials Research (DMR), National Science Foundation, under grant number NSF/CHE- 1834750. Use of the Advanced Photon Source, an Office of Science User Facility operated for the U.S. Department of Energy (DOE) Office of Science by Argonne National Laboratory, was supported by the U.S. DOE under Contract No. DE-AC02-06CH11357.

Data Availability Statement: Not applicable.

Acknowledgments: The contribution of all authors is gratefully acknowledged.

Conflicts of Interest: The authors declare no conflict of interest.

References

1. Pal, K.; Xia, Y.; Shen, J.; He, J.; Luo, Y.; Kanatzidis, M.G.; Wolverton, C. Accelerated Discovery of a Large Family of Quaternary Chalcogenides with Very Low Lattice Thermal Conductivity. *Npj Comput. Mater.* **2021**, *7*, 82. [CrossRef]

- 2. Patschke, R.; Zhang, X.; Singh, D.; Schindler, J.; Kannewurf, C.R.; Lowhorn, N.; Tritt, T.; Nolas, G.S.; Kanatzidis, M.G. Thermoelectric Properties and Electronic Structure of the Cage Compounds A2BaCu8Te10 (A = K, Rb, Cs): Systems with Low Thermal Conductivity. *Chem. Mater.* **2001**, *13*, 613–621. [CrossRef]
- 3. Qiu, P.; Shi, X.; Chen, L. Cu-Based Thermoelectric Materials. Energy Storage Mater. 2016, 3, 85–97. [CrossRef]
- 4. Wei, K.; Beauchemin, L.; Wang, H.; Porter, W.D.; Martin, J.; Nolas, G.S. Enhanced Thermoelectric Properties of Cu2ZnSnSe4 with Ga-Doping. *J. Alloys Compd.* **2015**, *650*, 844–847. [CrossRef]
- 5. Dong, Y.; Wang, H.; Nolas, G.S. Synthesis and Thermoelectric Properties of Cu Excess Cu2 ZnSnSe4. *Phys. Status Solidi-Rapid Res. Lett.* **2014**, *8*, 61–64. [CrossRef]
- 6. Dong, Y.; Wang, H.; Nolas, G.S. Synthesis, Crystal Structure, and High Temperature Transport Properties of p-Type Cu2Zn1-XFexSnSe4. *Inorg. Chem.* **2013**, 52, 14364–14367. [CrossRef]
- 7. Pal, K.; Singh, P.; Bhaduri, A.; Thapa, K.B. Current Challenges and Future Prospects for a Highly Efficient (>20%) Kesterite CZTS Solar Cell: A Review. *Sol. Energy Mater. Sol. Cells* **2019**, *196*, 138–156. [CrossRef]
- 8. Ravindiran, M.; Praveenkumar, C. Status Review and the Future Prospects of CZTS Based Solar Cell—A Novel Approach on the Device Structure and Material Modeling for CZTS Based Photovoltaic Device. *Renew. Sustain. Energy Rev.* **2018**, *94*, 317–329. [CrossRef]
- 9. Nolas, G.S.; Hassan, M.S.; Dong, Y.; Martin, J. Synthesis, Crystal Structure and Electrical Properties of the Tetrahedral Quaternary Chalcogenides CuM2InTe4 (M = Zn, Cd). *J. Solid State Chem.* **2016**, 242, 50–54. [CrossRef]
- 10. Sahu, M.; Minnam Reddy, V.R.; Park, C.; Sharma, P. Review Article on the Lattice Defect and Interface Loss Mechanisms in Kesterite Materials and Their Impact on Solar Cell Performance. *Sol. Energy* **2021**, 230, 13–58. [CrossRef]
- 11. Denisov, D.V.; Tsendin, K.D. Application of Chalcogenides for Creation of New Superconductors. *J. Optoelectron. Adv. Mater.* **2003**, *5*, 1011–1016.
- 12. Deguchi, K.; Takano, Y.; Mizuguchi, Y. Physics and Chemistry of Layered Chalcogenide Superconductors. *Sci. Technol. Adv. Mater.* **2012**, *13*, 054303. [CrossRef] [PubMed]

Crystals **2022**, 12, 1310 6 of 7

13. Mizuguchi, Y.; Takano, Y. Review of Fe Chalcogenides as the Simplest Fe-Based Superconductor. *J. Phys. Soc. Jpn.* **2010**, *79*, 102001. [CrossRef]

- 14. Feng, W.; Xiao, D.; Ding, J.; Yao, Y. Three-Dimensional Topological Insulators in I-III-VI2 and II-IV-V2 Chalcopyrite Semiconductors. *Phys. Rev. Lett.* **2011**, *106*, 016402. [CrossRef] [PubMed]
- 15. Chen, S.; Gong, X.G.; Duan, C.G.; Zhu, Z.Q.; Chu, J.H.; Walsh, A.; Yao, Y.G.; Ma, J.; Wei, S.H. Band Structure Engineering of Multinary Chalcogenide Topological Insulators. *Phys. Rev. B-Condens. Matter Mater. Phys.* **2011**, *83*, 245202. [CrossRef]
- 16. Xing, C.; Lei, Y.; Liu, M.; Wu, S.; He, W.; Zheng, Z. Environment-Friendly Cu-Based Thin Film Solar Cells: Materials, Devices and Charge Carrier Dynamics. *Phys. Chem. Phys.* **2021**, 23, 16469–16487. [CrossRef] [PubMed]
- 17. Tsiba Matondo, J.; Malouangou Maurice, D.; Chen, Q.; Bai, L.; Guli, M. Inorganic Copper-Based Hole Transport Materials for Perovskite Photovoltaics: Challenges in Normally Structured Cells, Advances in Photovoltaic Performance and Device Stability. *Sol. Energy Mater. Sol. Cells* **2021**, 224, 111011. [CrossRef]
- 18. Suresh, S.; Uhl, A.R. Present Status of Solution-Processing Routes for Cu(In,Ga)(S,Se)2 Solar Cell Absorbers. *Adv. Energy Mater.* **2021**, *11*, 2003743. [CrossRef]
- 19. Haque, E. Outstanding Thermoelectric Performance of MCu3X4(M = V, Nb, Ta; X = S, Se, Te) with Unaffected Band Degeneracy under Pressure. *ACS Appl. Energy Mater.* **2021**, *4*, 1942–1953. [CrossRef]
- 20. Chen, K.; Du, B.; Bonini, N.; Weber, C.; Yan, H.; Reece, M.J. Theory-Guided Synthesis of an Eco-Friendly and Low-Cost Copper Based Sulfide Thermoelectric Material. *J. Phys. Chem. C* **2016**, 120, 27135–27140. [CrossRef]
- 21. Skoug, E.J.; Cain, J.D.; Morelli, D.T. High Thermoelectric Figure of Merit in the Cu3SbSe4-Cu3SbS4 Solid Solution. *Appl. Phys. Lett.* **2011**, *98*, 261911. [CrossRef]
- 22. Ge, Z.H.; Salvador, J.R.; Nolas, G.S. Selective Synthesis of Cu₂SnSe₃ and Cu₂SnSe₄ Nanocrystals. *Inorg. Chem.* **2014**, *53*, 4445–4449. [CrossRef] [PubMed]
- 23. Boehnke, U.C.; Kühn, G. Phase Relations in the Ternary System Cu-In-Se. J. Mater. Sci. 1987, 22, 1635–1641. [CrossRef]
- 24. Manolikas, C.; van Landuyt, J.; de Ridder, R.; Amelinckx, S. Electron Microscopic Study of the Domain Structure and of the Transition State in Cu_{0.5}In_{2.5}Se₄. *Phys. Status Solidi* **1979**, *55*, 709–722. [CrossRef]
- 25. Folmer, J.C.W.; Turner, J.A.; Noufi, R.; Cohen, D. Structural and Solar Conversion Characteristics of the (Cu₂Se) x (In₂Se₃) 1 x System. *J. Electrochem. Soc.* **1985**, *13*2, 1319–1327. [CrossRef]
- 26. Rockett, A.; Birkmire, R.W. CuInSe₂ for Photovoltaic Applications. J. Appl. Phys. 1998, 70, R81. [CrossRef]
- Wang, K.; Qin, P.; Ge, Z.H.; Feng, J. Highly Enhanced Thermoelectric Properties of P-Type CuInSe₂ Alloys by the Vacancy Doping. Scr. Mater. 2018, 149, 88–92. [CrossRef]
- 28. Parlak, M.; Erçelebi, Ç.; Günal, I.; Özkan, H.; Gasanly, N.M.; Çulfaz, A. Crystal Data, Electrical Resisitivity and Mobility in Cu₃In₅Se₉ and Cu₃In₅Te₉ Single Crystals. *Cryst. Res. Technol.* **1997**, 32, 395–400. [CrossRef]
- 29. Rincón, C.; Wasim, S.M.; Marín, G.; Sánchez Pérez, G. Optical Absorption Spectra near the Fundamental Band Edge in Cu₂In₄Se₇ Bulk Crystals. *J. Appl. Phys.* **2003**, *93*, 8939. [CrossRef]
- 30. Merino, J.M.; Mahanty, S.; León, M.; Diaz, R.; Rueda, F.; Martin De Vidales, J.L. Structural Characterization of CuIn₂Se_{3.5}, CuIn₃Se₅ and CuIn₅Se₈ Compounds. *Thin Solid Films* **2000**, *361*–*362*, 70–73. [CrossRef]
- 31. Takei, K.; Maeda, T.; Gao, F.; Yamazoe, S.; Wada, T. Crystallographic and Optical Properties of CuInSe2-ZnSe System. *Jpn. J. Appl. Phys.* **2014**, *53*, 05FW07. [CrossRef]
- 32. Schorr, S.; Geandier, G. In-Situ Investigation of the Temperature Dependent Structural Phase Transition in CuInSe2 by Synchrotron Radiation. *Cryst. Res. Technol.* **2006**, *41*, 450–457. [CrossRef]
- 33. Li, S.; Zhao, Z.; Liu, Q.; Huang, L.; Wang, G.; Pan, D.; Zhang, H.; He, X. Alloyed (ZnSe)x(CuInSe2)1-x and CuInSexS2-x Nanocrystals with a Monophase Zinc Blende Structure over the Entire Composition Range. *Inorg. Chem.* **2011**, *50*, 11958–11964. [CrossRef] [PubMed]
- 34. Golovej, M.I.; Voroshilov, Y.V.; Potorii, M.V. Investigation of the System Cu(Ag,Tl)-B(V)-Se. *Izv. Vyss. Uchebn. Zaved. Khim. Khim. Tekhnol.* **1985**, 28, 7.
- 35. Fan, J.; Schnelle, W.; Antonyshyn, I.; Veremchuk, I.; Carrillo-Cabrera, W.; Shi, X.; Grin, Y.; Chen, L. Structural Evolvement and Thermoelectric Properties of Cu3—xSnxSe3 Compounds with Diamond-like Crystal Structures. *Dalt. Trans.* **2014**, *43*, 16788–16794. [CrossRef]
- 36. Pfitzner, A. Crystal Structure of Tricopper Tetraselenoantimonate (V), Cu3SbSe4. Z. Fur Krist.-New Cryst. Struct. 1994, 209, 685. [CrossRef]
- 37. Richard, V. Gaines Luzonite, Famatinite and Some Related Minerals. Am. Mineral. 1957, 42, 766-779.
- 38. Wei, S.H.; Ferreira, L.G.; Zunger, A. First-Principles Calculation of the Order-Disorder Transition in Chalcopyrite Semiconductors. *Phys. Rev. B* **1992**, *45*, 2533. [CrossRef]
- 39. Certain trade names and company products are mentioned in the text or identified in illustrations in order to adequately specify the experimental procedures and equipment used. In no case does such identification imply recommendation or endorsement by the National Institute of Standards and Technology.
- 40. Giannozzi, P.; Baroni, S.; Bonini, N.; Calandra, M.; Car, R.; Cavazzoni, C.; Ceresoli, D.; Chiarotti, G.L.; Cococcioni, M.; Dabo, I.; et al. QUANTUM ESPRESSO: A Modular and Open-Source Software Project for Quantum of Materials. *J. Phys. Condens. Matter* **2009**, 21, 395502. [CrossRef]
- 41. Blöchl, P.E. Projector Augmented-Wave Method. Phys. Rev. B 1994, 50, 17953–17979. [CrossRef]

Crystals **2022**, 12, 1310 7 of 7

42. Perdew, J.P.; Burke, K.; Ernzerhof, M. Generalized Gradient Approximation Made Simple [Phys. Rev. Lett. 77, 3865 (1996)]. Phys. Rev. Lett. 1997, 78, 1396. [CrossRef]

- 43. Perdew, J.P.; Ernzerhof, M.; Burke, K. Rationale for Mixing Exact Exchange with Density Functional Approximations. *J. Chem. Phys.* **1998**, 105, 9982. [CrossRef]
- 44. Cococcioni, M.; De Gironcoli, S. Linear Response Approach to the Calculation of the Effective Interaction Parameters in the LDA+U Method. *Phys. Rev. B-Condens. Matter Mater. Phys.* **2005**, *71*, 035105. [CrossRef]
- 45. Zhang, Y.; Xi, L.; Wang, Y.; Zhang, J.; Zhang, P.; Zhang, W. Electronic Properties of Energy Harvesting Cu-Chalcogenides: P-d Hybridization and d-Electron Localization. *Comput. Mater. Sci.* **2015**, *108*, 239–249. [CrossRef]
- 46. Hobbis, D.; Shi, W.; Popescu, A.; Wei, K.; Baumbach, R.E.; Wang, H.; Woods, L.M.; Nolas, G.S. Synthesis, Transport Properties and Electronic Structure of p-Type Cu1+: XMn2- XInTe4 (x = 0, 0.2, 0.3). *Dalt. Trans.* **2020**, *49*, 2273–2279. [CrossRef] [PubMed]
- 47. Momma, K.; Izumi, F. VESTA: A Three-Dimensional Visualization System for Electronic and Structural Analysis. *J. Appl. Crystallogr.* **2008**, *41*, 653–658. [CrossRef]
- 48. Roque Infante, E.; Delgado, J.M.; Lopez Rivera, S.A. Synthesis and Crystal Structure of Cu2FeSnSe4, a I2 II IV VI4 Semiconductor. *Mater. Lett.* **1997**, *33*, 67–70. [CrossRef]
- 49. Knight, K.S. The Crystal Structures of CuInSe2 and CuInTe2. Mater. Res. Bull. 1992, 27, 161–167. [CrossRef]
- 50. Hönle, W.; Kühn, G.; Neumann, H. Die Kristallstruktur von LiInSe2. Z. Für Anorg. Und Allg. Chem. 1986, 543, 161–168. [CrossRef]
- 51. Pauling, L.; Hultgren, R. The Crystal Structure of Sulvanite, Cu3VS4. Z. Für Krist.-Cryst. Mater. 1933, 84, 204–212. [CrossRef]
- 52. Van Arkel, A.E.; Crevecoeur, C. Quelques Sulfures et Séléniures Complexes. J. Less Common Met. 1963, 5, 177-180. [CrossRef]
- 53. White-Drayton, K.; Liu, S.; Moeller, K.D.; Bhowmik, A.; Hansen, H.A.; Vegge, T.; Hui, Y.; Chang, R.; Koumpouras, K.; Larsson, J.A. Distinguishing between Chemical Bonding and Physical Binding Using Electron Localization Function (ELF). *J. Phys. Condens. Matter* 2020, 32, 315502. [CrossRef]
- 54. Espinosa-García, W.F.; Ruiz-Tobón, C.M.; Osorio-Guillén, J.M. The Elastic and Bonding Properties of the Sulvanite Compounds: A First-Principles Study by Local and Semi-Local Functionals. *Phys. B Condens. Matter* **2011**, *406*, 3788–3793. [CrossRef]
- 55. Dong, Y.; Khabibullin, A.R.; Wei, K.; Ge, Z.-H.; Martin, J.; Salvador, J.R.; Woods, L.M.; Nolas, G.S. Synthesis, Transport Properties, and Electronic Structure of Cu2CdSnTe4. *Appl. Phys. Lett.* **2014**, *104*, 252107. [CrossRef]
- 56. Room temperature resistivity (0.07 mΩ-cm) was determined by utilizing a custom-built device to measure small crystals employing a two-point probe method.
- 57. Ali, M.A.; Jahan, N.; Islam, A.K.M.A. Sulvanite Compounds Cu3TMS4 (TM = V, Nb and Ta): Elastic, Electronic, Optical and Thermal Properties Using First-Principles Method. *J. Sci. Res.* **2015**, *6*, 407–419. [CrossRef]
- 58. Bougherara, K.; Litimein, F.; Khenata, R.; Uçgun, E.; Ocak, H.Y.; Uğur, S.; Uğur, G.; Reshak, A.H.; Soyalp, F.; Omran, S.B. Structural, Elastic, Electronic and Optical Properties of Cu3TMSe4 (TM = V, Nb and Ta) Sulvanite Compounds via First-Principles Calculations. *Sci. Adv. Mater.* **2013**, *5*, 97–106. [CrossRef]
- 59. Liu, M.; Lai, C.Y.; Zhang, M.; Radu, D.R. Cascade Synthesis and Optoelectronic Applications of Intermediate Bandgap Cu3VSe4 Nanosheets. *Sci. Rep.* **2020**, *10*, 21679. [CrossRef] [PubMed]
- 60. Syu, W.J.; Hsu, R.Y.; Lin, Y.C. Growth and Photovoltaic Device Using Cu3VS4 Films Prepared via Co-Sputtering from Cu–V and V Targets. *Mater. Chem. Phys.* **2022**, 277, 125547. [CrossRef]